

Cubic PdNPs-based Air-breathing Cathodes Integrated in Glucose Hybrid Biofuel Cells

Deonildo Faggion Junior^{1,2,3}, Raoudha Haddad^{2,3}, Fabien Giroud^{2,3}, Michael Holzinger^{2,3}, Carlos Eduardo Maduro de Campos⁴, Jose Javier S. Acuña⁵, Josiel B. Domingos^{1*}, Serge Cosnier^{2,3*}

¹Chemistry Department, Universidade Federal de Santa Catarina, Trindade Campus, Florianópolis, SC, 8040-900, Brazil

²Univ. Grenoble Alpes DCM UMR 5250, F 38000, Grenoble, France

³CNRS, DCM UMR 5250, F-38000 Grenoble, France

⁴Physics Department, Universidade Federal de Santa Catarina, Trindade Campus, Florianópolis, SC, 88040-900, Brazil

⁵Centro de Ciências Naturais e Humanas, Universidade Federal do ABC, Santo André, SP, 09210-170, Brazil

Keywords: Cubic palladium nanoparticles, oxygen reduction, electrocatalysis, hybrid-biofuel cells

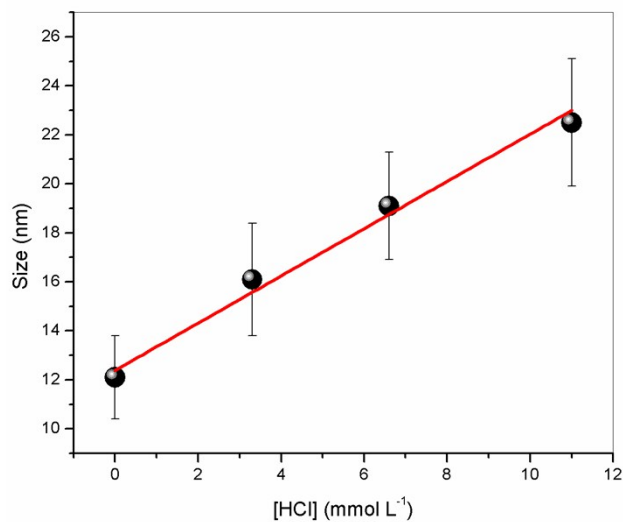


Figure S1: Linear correlation of the PdNPs sizes with the HCl concentration used in the synthesis of the cubic PdNPs ($R^2 = 0.98$).

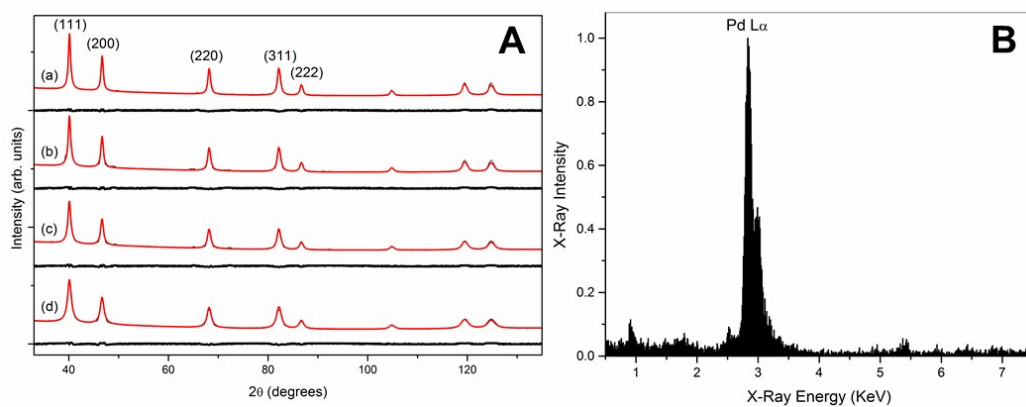


Figure S2: (A) Experimental (red lines) and difference between experimental and calculated (black lines) XRD patterns of the cubic PdNPs of (a) 22.5 nm, (b) 19.1 nm, (c) 16.1 nm and (d) 12.1 nm and (B) Representative EDS spectrum of cubic PdNPs of 12.1 nm.

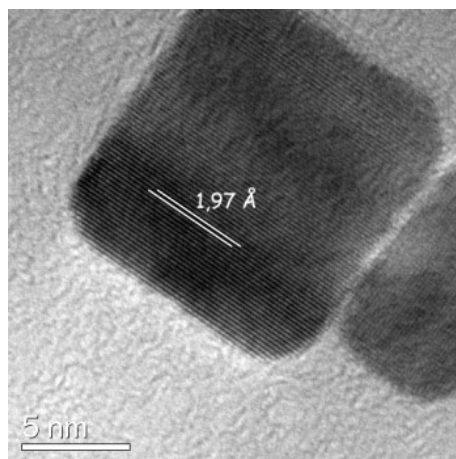


Figure S3: HRTEM image of a single cubic PdNP.

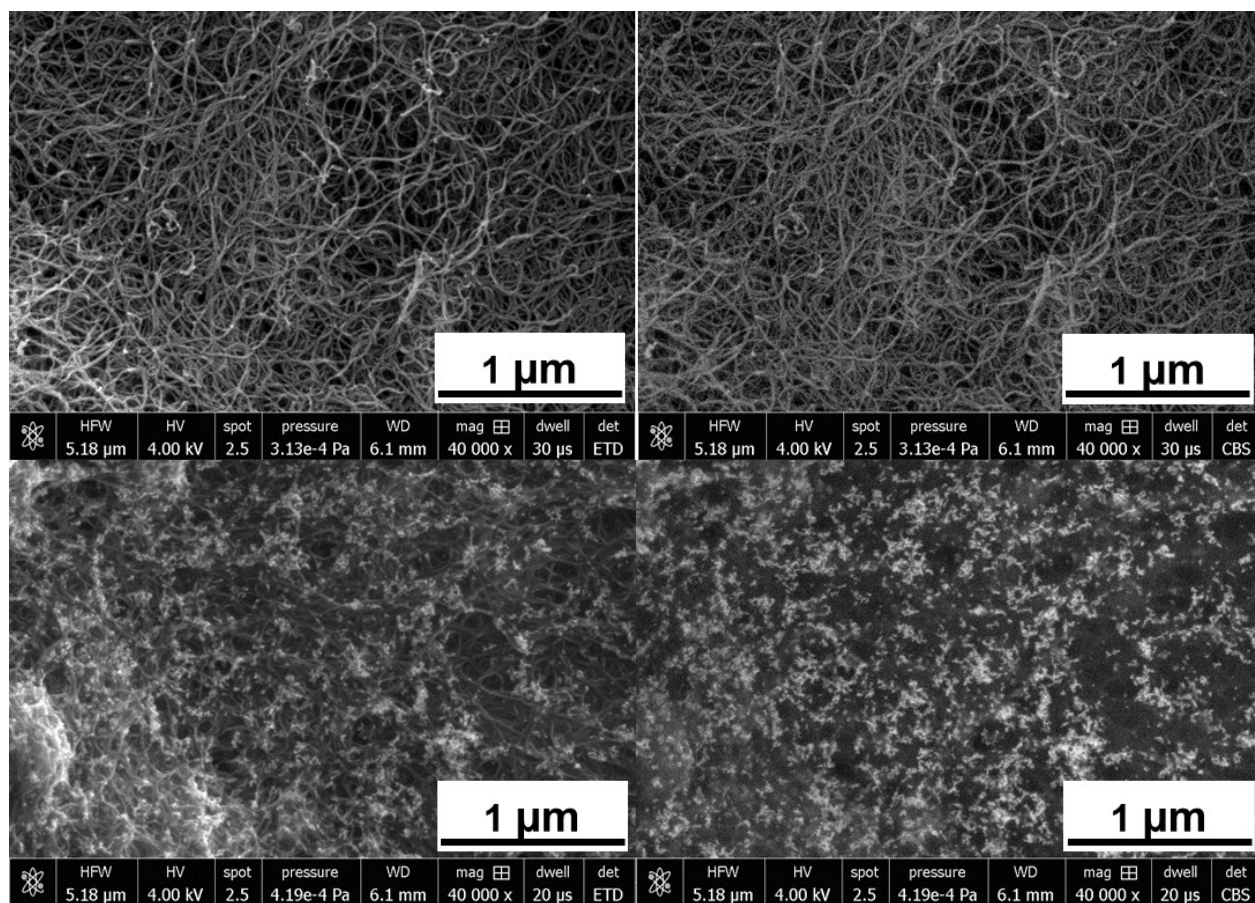


Figure S4: SEM images of the MWCNT (**up**) MWCNT/cubic PdNPs composites (**down**). The images were recorded from the same sampled area at different detection modes using a (**left**) secondary electron detector (Everhart-Thornley; ETD) to focus the in-depth visualization of the MWCNT deposit and (**right**) backscattered electron detector (CBS) for better contrast of the PdNPs distribution on the MWCNTs.

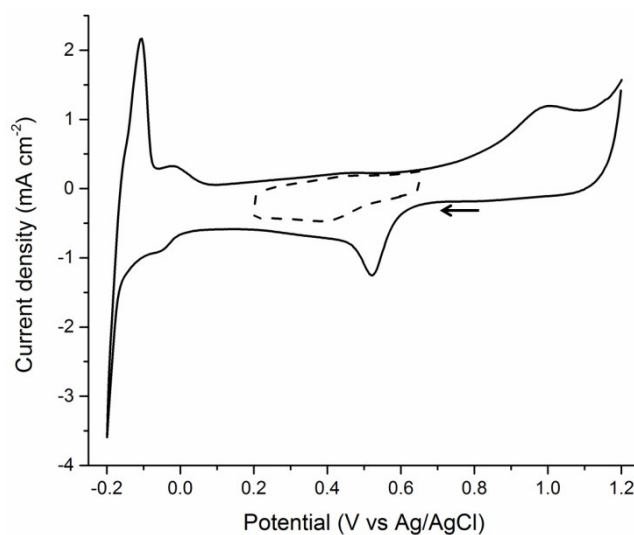


Figure S5: Cyclic voltammograms of PdNPs/MWCNT-modified GC electrode in 0.1 mol L⁻¹ H₂SO₄ solution at room temperature and Ar saturated condition: (dash) restrained and (line) extended electrochemical window, scan rate 10 mVs⁻¹. For clarity, only third cycles are presented here.

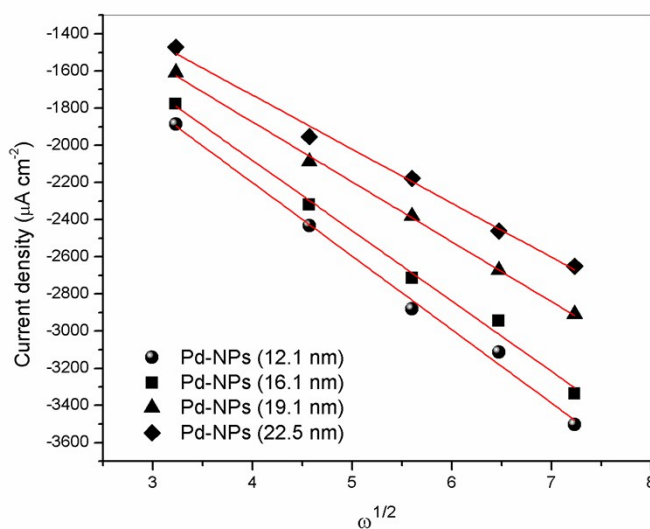


Figure S6: Linear correlation between the current and the speed of revolution for each size of cubic PdNPs for PdNPs/MWCNT-based electrodes. Data recorded and extracted from CV experiments at -0.4 V (McIlvaine buffer pH 6.0)

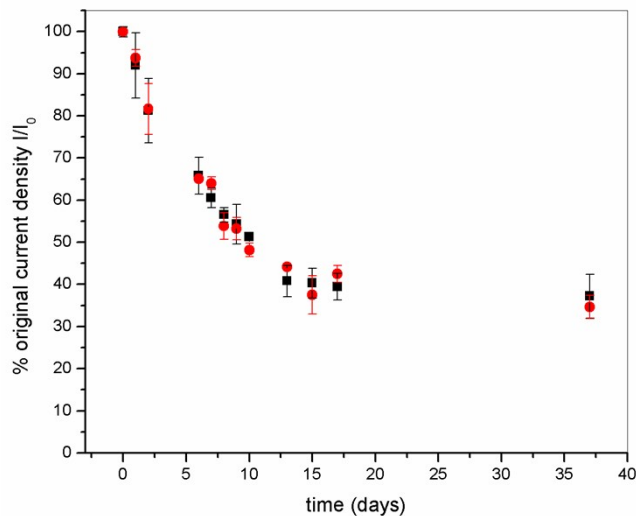


Figure S7: Relative current value (I/I_0) vs time for different storage conditions at room temperature: in open air (**black**) and in McIlvaine buffer pH 6.0 (**red**). Current was extracted from CV experiments at 0.0 V vs. Ag/AgCl at 10 mV s^{-1} .

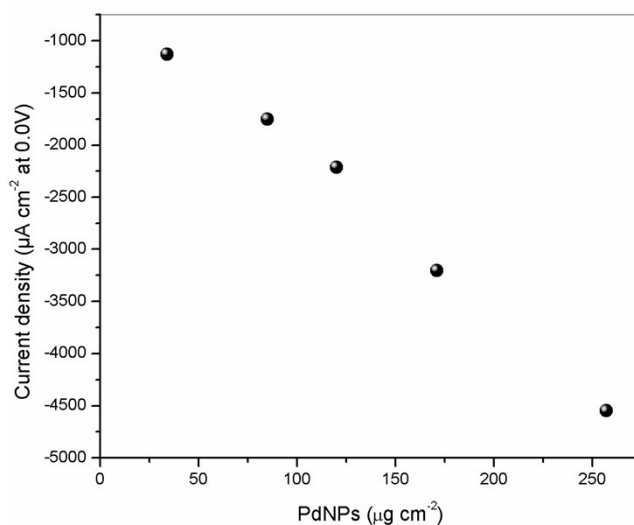


Figure S8: Different loads of cubic PdNPs ($\mu\text{g cm}^{-2}$), and the current ($\mu\text{A cm}^{-2}$) at 0.0 V from cyclic voltammograms in McIlvaine buffer (pH 6.0) and scan rate of 5 mV s^{-1} , tested under a PdNPs/MWCNT-modified GDL electrode. Only 12.1 nm PdNPs were evaluated here.

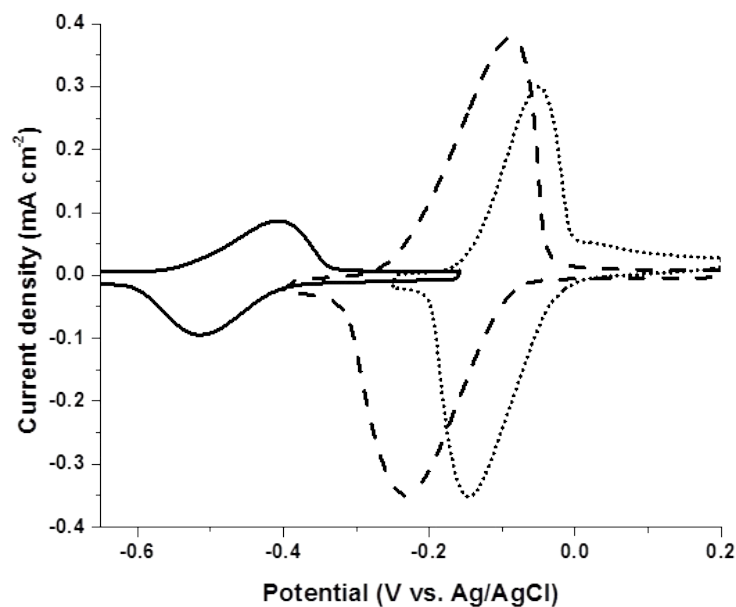


Figure S9: Representative cyclic voltammograms of different adsorbed quinones onto MWCNTs-based electrodes in pH 7.0 McIlvaine buffer (pH 7.0) at 10 mV s⁻¹. AQS (line), PQ (dash) and PLQ (dot).

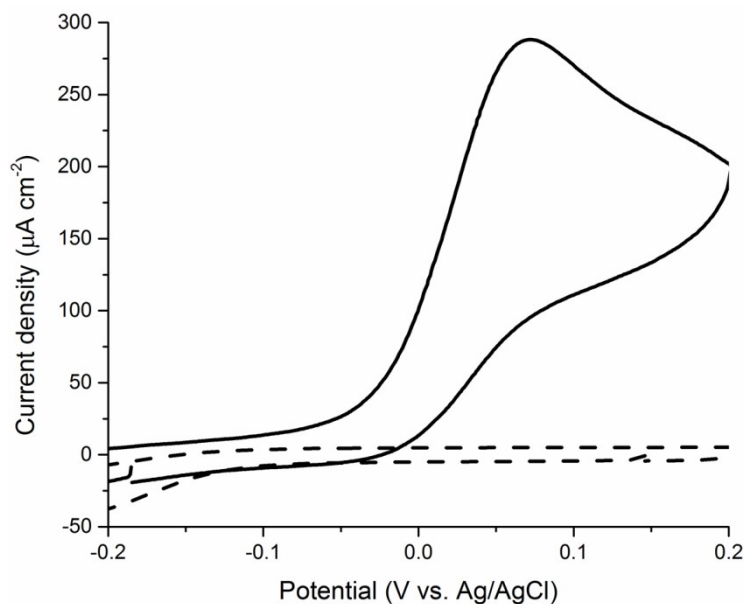


Figure S10: Representative cyclic voltammograms of unmodified MWCNTs-based electrodes in McIlvaine buffer (pH 7.0) at 5 mV s⁻¹ in absence (line) and presence (dash) of 2 mmol L⁻¹ NADH.

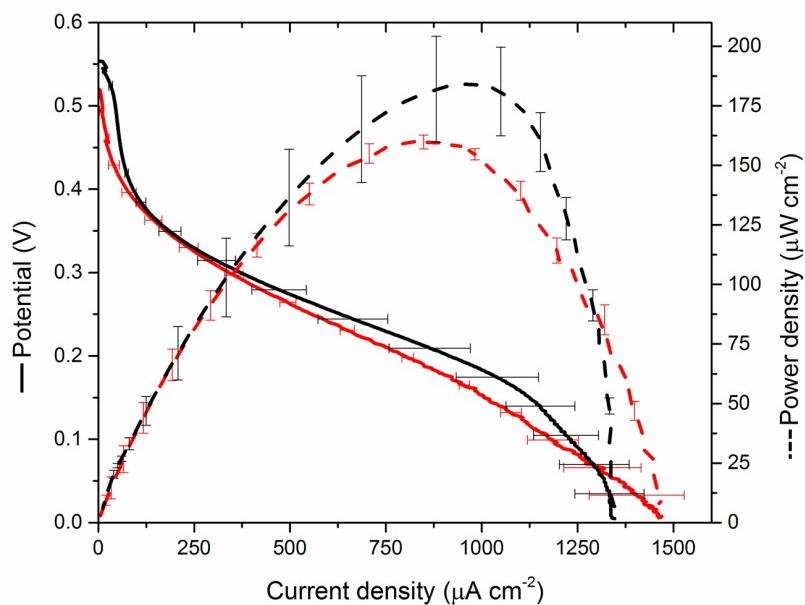


Figure S11: Polarization (solid line) and power (dashed line) curves obtained from PdNPs/MWCNT/GDL-air breathing cathode (**black**), and PdNPs/MWCNT/GC cathode under constant O_2 flow (**red**), both combined with a PLQ/pyrGDH/GC modified anode in a hybrid biofuel cells, in presence of $2 \text{ mmol L}^{-1} \text{ NAD}^+$ and 50 mmol L^{-1} glucose, in McIlvaine buffer (pH 7.0). Linear sweep voltammetry was recorded at 1 mV s^{-1} .